

Efficient Production of Platelets from Umbilical Cord Blood Stem Cells Using A Collagen-Tragacanth Scaffold in A Multi-Chamber Bioreactor

Mohamad Hosein Derakhti Gonbad, PhD student ¹, Ali Baradar Khoshfetrat, PhD ², Ali Akbar Movassaghpuor, PhD ³, Zohre Sanaat, MD³, Hojjatollah Nozad Charoudeh, PhD ^{4*}

1. Applied Cell Sciences Department, Advanced Research Medical School, Tabriz University of Medical Sciences, Tabriz, Iran.

2. Chemical Engineering Faculty, Sahand University of Technology, Tabriz, Iran.

3. Hematology and Oncology Research Center, Tabriz University of Medical Sciences, Tabriz, Iran.

4. Drug Applied Research Center, Tabriz University of Medical Sciences, Tabriz, Iran.

*Corresponding author: Dr. Nozad Charoudeh Hojjatollah, Golgasht Street, Drug Applied Research Center, Tabriz University of Medical Sciences, Tabriz, Iran, Email: nozadh@tbzmed.ac.ir, ORCID ID: 0000-0003-04883-9924

Received: 07 January 2023

Accepted: 25 April 2023

Abstract

Background: To date, platelet (PLT) transfusion is the main medical option for the treatment of thrombocytopenia. Nowadays, allogenic PLTs are commonly used for blood donation. Due to the limitations in the preparation and storage of PLTs, researchers try to develop alternative modalities such as bioreactors for the in-vitro expansion and production of PLTs for therapeutic purposes by promoting the differentiation of different types of stem cells into megakaryocytes (MK) and PLTs.

Materials and Methods: In this experimental study, umbilical cord blood stem cells (UCB-SC) were differentiated into MK. To this end, a new bioreactor system consisting of six compartments and a two-layer scaffold made of collagen and natural tragacanth gum was developed to mimic a bone marrow-like structure. After MKs were loaded to the top layer of the scaffold, the production rate of PLTs was analyzed under shear stress.

Results: Based on the estimation, each MK produced about 17.42 PLTs loaded into the scaffold collagen. This value emerged to be 23.46 and 9.44 PLTs in the collagen-tragacanth and the pure tragacanth scaffold groups, respectively, the increase of PLTs in the collagen-tragacanth scaffold was statistically significant ($p < 0.001$). The generated PLTs had a positive response in aggregometry as well as interaction with normal PLTs.

Conclusion: Taken together, the designed bioreactor with a collagen-tragacanth substrate can be used for the production of a sufficient number of PLTs for clinical purposes.

Keywords: Bioreactor, Megakaryocyte, Platelet, Scaffold, Tragacanth

Introduction

Besides maintaining vascular endothelial integrity, platelets (PLTs), as cellular particles, play a key role in forming a “PLT plug” and inducing coagulation homeostasis. PLTs are produced from megakaryocytes (MK) in the bone marrow (BM) through a process called thrombopoiesis or thrombocytopoiesis in which each MK may shed 2000 to 10000 PLTs (1, 2). The cytoplasmic fragmentation of MKs and the formation of PLTs are tightly controlled by numerous internal factors, along with the interaction of MKs with juxtaposed cells, either homotypic and heterotypic cells, and

the surrounding matrix (cell-to-matrix). It is suggested that the mutual interaction of MKs with the endothelial layer results in the release of PLTs into circulation (2–4). Thrombocytopenia is one of the major life-threatening challenges that can occur in some pathological conditions such as aplasia, leukemia, chemo or radiotherapies, and immunological diseases associated with PLT transfusion (2, 5, 6). Limited access to adequate PLT sources, short-term PLT storage (about 3-5 days), higher infection possibility, and higher pH variation are the most challenging issues in the preparation of PLTs for all blood product providers. In

this regard, researchers have tried to produce large amounts of PLTs in laboratory settings (2). It is to be noted that the majority of conventional culture systems cannot produce enough PLTs. This is due to the lack of physical interactions between cells and matrix materials and the shear stress which are necessary for PLT production. It is thought that these parameters can be completely provided in 3D culture systems and more efficiently inside a bioreactor (7, 8). The applied 3D structures should be accessible, biocompatible, and cost-effective enough to produce clinically acceptable PLTs (1, 2, 4, 9, 10). Scaffolds made from collagen, silk, and other artificial materials have been utilized in previous studies. However, the high price of collagen, relatively hard production process, adverse effects of silk on PLTs' function, and loose interaction between MKs and artificial matrix materials discourage their application in PLT bioprocessing (1, 3, 11).

In recent years, PLT production from hematopoietic stem cells (HSCs), peripheral blood (PB) stem cells (PBSC), UCB-SCs, adipose-derived mesenchymal stem/stromal cells (ASCs), and induced pluripotent stem cells (iPSCs) in in vitro conditions has been considered to be of advantages and disadvantages (1,12–18). For instance, cord blood CD34+ and CD133+ cells can be differentiated into MKs. High source availability and low antigenicity are the major advantages of cord blood samples (2, 19). The ploidy status of the MKs differentiated from UCB-SCs and its positive effect on the amount of PLT production through conventional culturing methods have already been demonstrated (1, 2). The application of ploidy enhancer factors such as actin polymerization inhibitor latrunculin B and Rho-kinase inhibitor can affect the dynamic growth of MKs and PLTs (20). Therefore, in this research, an attempt is made to increase production chambers and minimize cell manipulation to produce more functional and a greater

number of PLTs from UCB-SCs in a collagen-tragacanth scaffold. Tragacanth was used as an extracellular matrix agent along with collagen. This substrate is a natural one with a high-quality hydrocolloid, and it has been used in different studies for drug delivery, wound healing, bio-protection, tissue scaffolding, and cell culturing (15, 21–24). Tragacanth is a natural gum derived from the *Astragalus gossypinus* plant, known as tragacanth gum (TG). It has a polysaccharide structure with a small amount of protein and has recently been shown as a promising therapeutic substance in tissue engineering and regenerative medicine. This polymer is known to be biodegradable, non-allergenic, non-toxic, and non-carcinogenic. The stability of TG against microbial effects, heat, and acid degradation has made it an attractive material in industrial settings and biomedical approaches (25, 26). As a biological material, TG is safe for eukaryotic cells (27). A combination of collagen and TG can be used as a substitute for the BM extracellular matrix. It is advantageous because of numerous polysaccharides residues, glycosaminoglycans-like hyaluronic acid, proteoglycans, and glycoproteins with profound effects on megakaryopoiesis and thrombopoiesis processes. A 2-layer collagen scaffold was integrated into a novel multi-chamber (6-chamber) bioreactor culture system, whereby one side of the chamber would allow the seeding of cultured UCB-SCs-derived MKs into scaffold cross-flows and subject them to shear forces to induce PLT release into a parallel collecting flow. The bioreactor-derived PLTs were examined for its normal cell structure and functional abilities (28).

Materials and Methods

Tragacanth gum

This material is extracted from a plant called *Astragalus*. Astragal is a high-

quality hydrocolloid and is chemically produced from two non-homogenous branched hydrophilic carbohydrates, namely Bassorin and Tragacanthin. Bassorin forms almost 60-70% of the gum's composition, absorbs water, and swells to form a very viscous gel-like structure (29). It is an insoluble component of the gel, but the soluble components of TG (Tragacanthin) are dissolved in water to create a thick colloidal hydrosol. The acidic part of the composition produces some D-Xylose, L-Fucose, and D-Galacturonic acid through acidic hydrolysis. Tragacanthin is already isolated in ethanol-soluble (arabinogalactan) and insoluble (tragacanthic acid) sub-fractions. It is composed of Tragacanthic acid with residues of D-galacturonic acid, D-galactose, L-fucose and D-xylose as well as arabinogalactan, which contains residues of D-galactose, L-arabinose and D-galacturonic acid. This material is soluble in water and finally produces a colloid form. The final properties of astragal are due to the function of Basurin (15, 21, 22, 24, 29).

Designing the scaffold

In the present study, a two-step freezing method was used to generate a multilayer scaffold. To this end, 3 ml of 1% collagen (w/v) (prepared in the chemistry department of Sahand University of Technology, Tabriz) was poured into each well of 24-well plates after filtration (0.41 μm Whatman filter) and freezing at -20°C for an hour. Then, the plate was incubated at room temperature (RT) for 5 minutes for partial melting. The second collagen layer was purred up to 3.5-mm thickness above the first layer and frozen at -40°C for an hour. Thereafter, the plate was freeze-dried for 24 hours. Collagen crosslinking was done by using EDC/NHS [1-Ethyl-3-(3'-dimethyl-aminopropyl) carbodiimide/N Hydroxysulfosuccinimide sodium] (Sigma-Aldrich) for an hour. To continue the procedure, the scaffold was washed three times with distilled water for 15

minutes (30). Finally, the plate was again freeze-dried for 24 hours and stored at -20°C until use (31–33). To create a collagen-tragacanth scaffold, 1% collagen and 1% Tragacanth were mixed at a 1:1 ratio. For a scaffold with tragacanth alone, 2% tragacanth was used in the mentioned steps. In this group, 2% glutaraldehyde (Sigma-Aldrich) was used at a 1:1 ratio to cross-link tragacanth. Finally, to examine the pore size of the scaffold, SEM images were taken of the top and bottom layers (Figure 1).

To ensure the scaffold function in the bioreactor, PB blasts were isolated from patients with leukemia AML (M5) and injected into the upper layer of the scaffold. Then, the number of the blasts released from the lower layer was examined. These blasts were homogeneous and approximately of the same size (20 μm) as the cultured MKs. A PLT suspension of normal individuals was also used to examine the passage of PLTs from the lower layer.

Multi-chamber bioreactor design

A multi-chamber (6-chamber) bioreactor was designed with polycarbonate that had low interaction with PLTs. The main compartment of the bioreactor was designed in the form of two complementary plates, each of which has six chambers with a diameter of 5 mm. The chambers were connected through 1-mm narrow channels. These compartments were custom-made from polycarbonate to provide a flexible polymer surface with low PLT reactivity. Each plate had an inlet and an outlet. In the upper plate, the inlet and outlet were connected to the culture medium tank through a polyvinyl chloride (PVC) pipe, and a peristaltic pump flow rate was induced. The inlet of the lower plate was connected to the tank of the culture medium, and its outlet was connected to a blood bag. The fixtures and fittings were made of medical-grade polypropylene and PVC tubing to reduce the exposure of cells to charged surfaces or

cell reaction surfaces. The flow in the channels before and after the bioreactor was externally regulated away from the flow chamber by the addition of pinch valves and restrictions. Also, six two-layered collagen scaffolds of $5 \times 5 \times 3$ mm were attached to a PVC holding frame in the bioreactor system with 6×6 -mm diaphragms on the upper and lower surfaces. The upper layer of collagen had large pores for MK. In contrast, the lower layer of the scaffold had small pores that would allow only PLTs to pass through. A 10-cm polydimethylsiloxane (PDMS) tube was placed before and after the chamber to provide a gas exchange. This bioreactor design created stable parallel flow and, as a result, shear stress on the surfaces of the collagen scaffold (Figure 2).

Mononuclear cells (MNCs) and CD34+ cells enrichment

Initially, 20 ml of umbilical cord blood (UCB) was collected during normal deliveries under sterile conditions. All the volunteers were asked to fill out informed consent. The samples were collected in 50-ml conical tubes with 500 IU heparin (Caspian Tamin). After that, the UCB samples were diluted with phosphate buffer saline (PBS, Life Technologies, Carlsbad, CA) at a 2:1 ratio. The procedure was continued by the centrifugation of the samples at 850 g and 4°C for 25 minutes to collect MNCs. Subsequently, the MNCs were isolated using the Ficoll-Hypaque gradient (GE Healthcare, Barrington, IL). The MNCs at the interface were isolated, and the RBCs were collected in the other conical tubes, and washed with PBS and 10% fetal bovine serum (FBS, Life Technologies) at 600 g. In this study, the average number of the harvested MNCs was about $3 \times 10^7/\text{ml}$. Using the MACS method, the CD34+ cells were enriched according to the manufacturer's instructions (Mini MACS, Miltenyi Biotech, Auburn, CA) (2, 19, 20).

Megakaryocytic differentiation and PLT production in the bioreactor system

In this section of the study, about $1 \times 10^4/\text{ml}$ umbilical cord blood stem cells (UCB-SC) were cultured in the Roswell Park Memorial Institute (RPMI) 1640 culture medium. To induce megakaryocytic differentiation, 50 ng/ml thrombopoietin (TPO; Bio-Techne) and 5 ngr/ml stem cell factor (SCF, Gibco) were added to the culture medium. On day 8, the complete RPMI1640 culture medium was replenished by the addition of 50 ng/ml TPO. The concentration of the differentiated cells was raised to 1×10^6 , and then the cells were cultivated for the subsequent 3-4 days (20).

A multi-chamber (6-chamber) bioreactor was designed from polycarbonate with minimal interaction with PLTs. Each one of the six chambers contained a piece of two-layer collagen scaffold, 5 mm in diameter and 3 mm in thickness, cut by a specific cutter. Each chamber was also separated by a gasket to prepare a channel for the medium flow. The upper chamber was connected to a medium reservoir and a CO_2 pump, and the lower chamber was connected to a bag of CPDA-1 through propylene tubes so as to harvest the released PLTs (Figure 2). Before starting, the bioreactor system was treated with 5 ml of PBS by gravity feed, 5 ml of PBS to rinse the system, and 5 ml of a blocking solution of RPMI1640 containing 0.01% BSA (bovine serum albumin) for 30 minutes. It was followed by thorough rinsing in PBS and washing with 5 ml of RPMI1640 culture medium twice for five minutes.

Approximately, 1×10^4 CD41+ cells were seeded on the upper layer of each scaffold, and 5 ml of RPMI1640 medium was slowly added to each chamber. Thereafter, the chamber was closed, and the bioreactor started working at 37°C for an hour at a flow rate of 30-70 $\mu\text{l}/\text{sec}$ with 5% CO_2 (33). The final harvested PLTs were counted with an automatic cell-counting system

(Sysmex kx 21). Manual counting was also done to confirm the automated count and check the possibility of PLT aggregation using the Neubauer slide. Light microscopy and Giemsa staining were conducted for the morphological analysis of the produced MKs differentiated from UCB-SC and pro-PLTs on days 11 and 14, respectively. The PLTs collected from the bioreactor were stained with Giemsa (Fisher Scientific) and observed with a light microscope connected to a camera (Figure 4).

Flow cytometric evaluations of MKs and the produced PLTs

To evaluate the megakaryocytic differentiation, 10^5 cells were washed with PBS and then incubated with 10 μ l of FITC conjugated anti-CD41 (Sigma-Aldrich) for an hour. The cells were washed with PBS and re-suspended in 500 μ l of 5% BSA-containing PBS. The evaluations were done by a BD FACSCalibur flow cytometry system (BD, USA). To confirm the PLT phenotype, the particles were incubated with 10 μ l of anti-CD41-FITC and 10 μ l of anti-CD42-PE (Sigma-Aldrich) antibodies, washed with PBS, and re-suspended in a 5% BSA-PBS solution and then evaluated as previously described (11,12,17,18, 33–35).

Functional evaluations of the PLTs

The aggregometry technique served to examine the PLT aggregation in platelet-rich plasma (PRP). This was done with certain agonists including ADP (0.5–10 μ m), Ca^{+2} (1mmol/l), collagen (0.5–10mg/ μ L), ristocetin (0.75–1.25mg/mL) and arachidonic acid (0.12–1.0mm). The PLT agonists were purchased from Hyphen Biomed, and an aggregometer [chronology model 700 x, Havertown, Pennsylvania (PA)] was used as the reference instrument (1, 36–39). To investigate the interaction of bioreactor PLTs with natural PLTs, normal donor PLTs were stained with 3,3'-dihexyloxacarbocyanine iodide (DIOC6;

green, Thermo Fisher Scientific), and the bioreactor PLTs were stained with Cell Tracker™ Red (Thermo Fisher Scientific) and stimulated by being passed through a high-pressure collagen-coated microtubule. Also, an immunofluorescence microscope served to monitor and image the PLT aggregation (Figure 4) (33).

Ethical considerations

This study was approved by the Academic Research Ethics Committee of Tabriz University of Medical Sciences (code of ethics: IR.TBZMED.REC.1397.610).

Statistical analysis

All the tests were repeated three times, and the normality of the data was investigated with the Shapiro-Wilk test. The levels of statistical significance were determined either through analysis of variance or with Tukey post-hoc test, and $p < 0.05$ was considered significant. The SPSS software version 24 was also used for the data analysis.

Results

Properties of the constructed scaffold

In this study, a collagen scaffold was made with a bi-phasic technique. The first and the lower phase was frozen at $-20^{\circ}C$ with a pore size ranging from 10 μ m to 30 μ m to prohibit MKs from passing. The second and the upper phase was frozen at $-40^{\circ}C$ to produce a large pore size of 50–100 μ m to allow MKs to pass easily. The function of the scaffold in filtering the cells was evaluated with WBCs from the buffy coats of AML-M5 patients. This is because the blast cells in AML-M5 were the same size as the cultured MKs. About 10^5 AML blasts were introduced to the scaffold, and nearly all were trapped in the top layer. More than 90% of the cells were retrieved. To evaluate the PLTs passing through the scaffold, 2×10^6 PLTs were injected into the scaffold. More than 90% of the injected PLTs passed through.

In the scaffold composed of collagen and tragacanth and the one with tragacanth

alone, the lower (-20°C treatment) and upper (-40°C treatment) phases were completely different in pore size. In the upper part, large cavities were postulated for the easy placement of MKs. In the lower part, small cavities were provided to prevent MKs from passing and allow PLTs to pass easily. Figure 1 presents the corresponding SEM images.

Differentiation and expansion of MKs

The purity of the enriched CD34+ cells reached $71.2 \pm 8\%$ after MACS sorting and flow cytometric analysis (Figure 3). On average, the number of the cells increased from the initial concentration of $1.5 \times 10^5/\text{ml}$ to $18.6 \pm 2.5 \times 10^6/\text{ml}$ cells after 11 days, and about $64.4 \pm 5\%$ of these cells expressed CD41. This change indicated the differentiation and proliferation of MKs (for about 80 folds) in the presence of SCF and TPO (Figure 3).

Countable quantity of the PLTs produced in the bioreactor

Approximately 1×10^4 cells (6×10^4 cells in six chambers) were seeded at the top layer of the scaffold with the bioreactor running at a 30-70ml/min rate for 30 minutes. The platelet-like particles (PLPs) were isolated under shear stress in the lower chamber. About $1.045 \pm 0.073 \times 10^6$ PLPs were collected from the collagen scaffold. The corresponding values were $1.408 \pm 0.087 \times 10^6$ and $0.566 \pm 0.053 \times 10^6$ in the collagen-tragacanth scaffold and the one with tragacanth alone. The increase of PLTs ($\times 1000$) in the collagen-

tragacanth scaffold was statistically significant ($p < 0.001$) (Table I). They were collected in blood bags containing CPD-A1. As estimated, each MK generated 17.42 ± 1.23 , 23.46 ± 1.44 and 9.44 ± 0.88 PLTs after loading into collagen, collagen-tragacanth, and pure tragacanth. The increase of PLTs (PLTs per MK) in the collagen-tragacanth scaffold was statistically significant ($p < 0.001$) (Table I). The flow rate at the outlet pipe was set at $0.1 \mu\text{l}/\text{min}$ to control the bioreactor, where the flow of the medium occurred spontaneously without PLT particle isolation (Figure 3).

Considerable properties of the produced PLTs

The PLTs produced for surface markers were evaluated by flow cytometry in terms of CD41 and CD42. Based on the data, the expression rates of CD41 and CD42 in the isolated PLTs were 95.2% and 96.3%, respectively. Giemsa staining was done to evaluate the morphology, size, structure, and granulation of the platelets. The morphology of the cells was normal. An aggregometric technique also revealed the rather acceptable activity of the cells (Figures 3 and 4). Normal individual PLTs were stained with DIOC6 (green), and bioreactor PLTs were stained with Cell Tracker™ Red and then stimulated by being passed through a high-pressure collagen-coated microtubule. Notably, both normal and bioreactor PLTs participated in the formation of PLT aggregates (Figure 4).

Table I. Mean and standard deviation of the number of PLTs (x1000) and the PLT count (PLTs per-MK) produced in the bioreactor in different scaffold groups

Scaffold groups	PLTs (x1000)			PLT count (PLTs per-MK)		
	Mean ± SD	F	p-value	Mean ± SD	F	p-value
Collagen	1045.20 ± 73.53	168.69	< 0.001	17.42 ± 1.23	170.217	< 0.001
Collagen-tragacanth	1408 ± 87.03			23.46 ± 1.44		
Tragacanth	566.20 ± 53.58			9.44 ± 0.88		

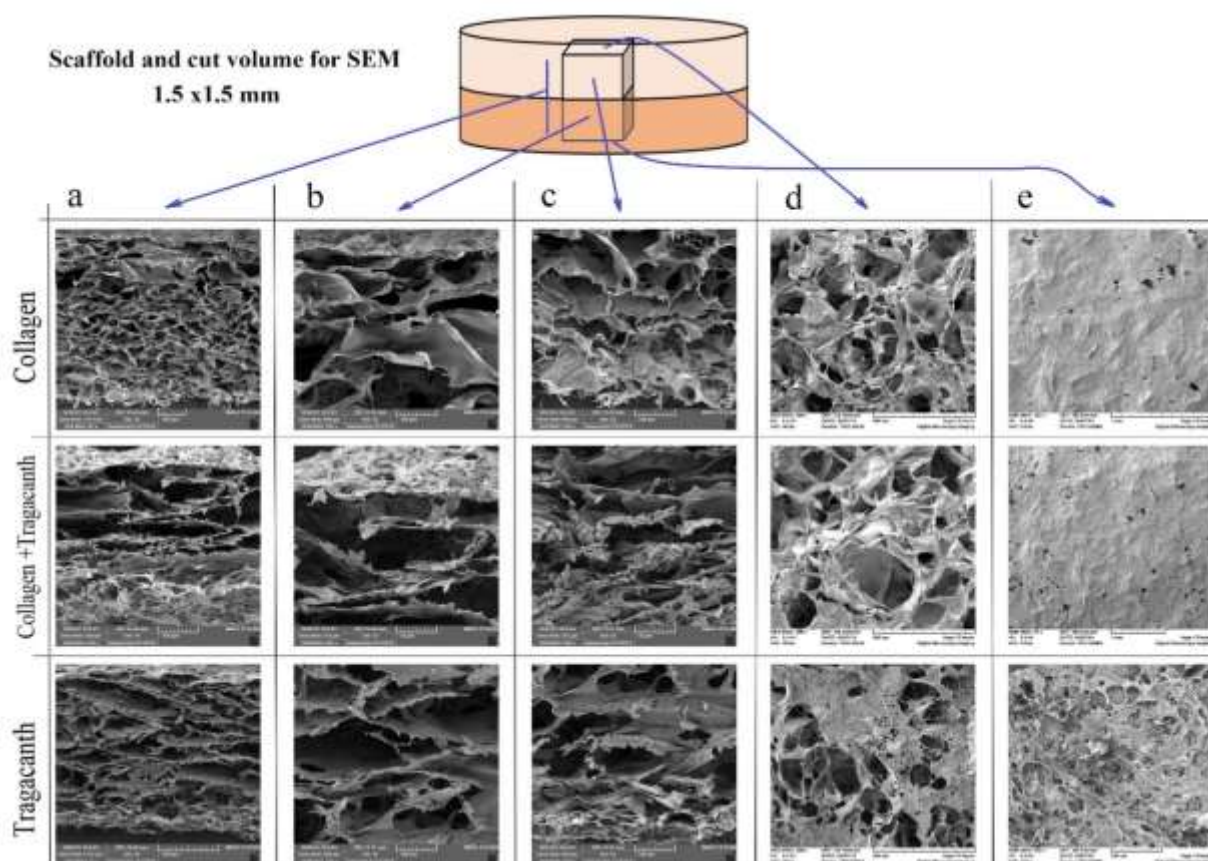


Figure 1. Electron microscopy of collagen, collagen-tragacanth, and tragacanth scaffolds: a. Both upper and lower phases of the scaffold, b. The upper side of the scaffold where the large pore for MKs is located, c. The lower side of the scaffold where tiny pores block the passage of MKs, d. The top of the scaffold where there are very large pores for MKs to pass, e. The bottom of the scaffold where very small cavities only allow PLTs to pass through

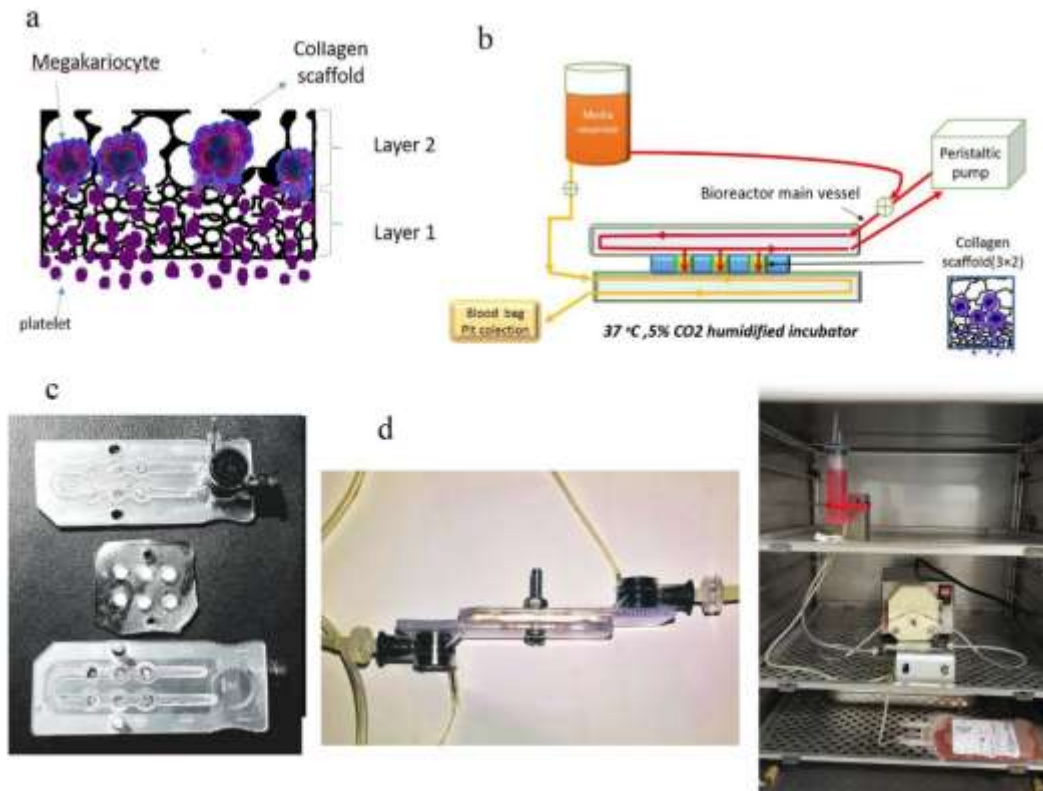


Figure 2. The scheme and steps of designing a multi-chamber (six-chamber) bioreactor: a. The scheme of the platelet production in the scaffold, b. The outline of the bioreactor function, c. Two plates for media flow and six chambers (The upper plate is connected to the medium pump, and the bottom plate is attached to the culture medium reservoir on one side and to the blood bag containing CPD-A1 on the other side. These two plates were separated by a plastic lining.), d. Connection of two layers with screws, e. A completely assembled bioreactor in an incubator

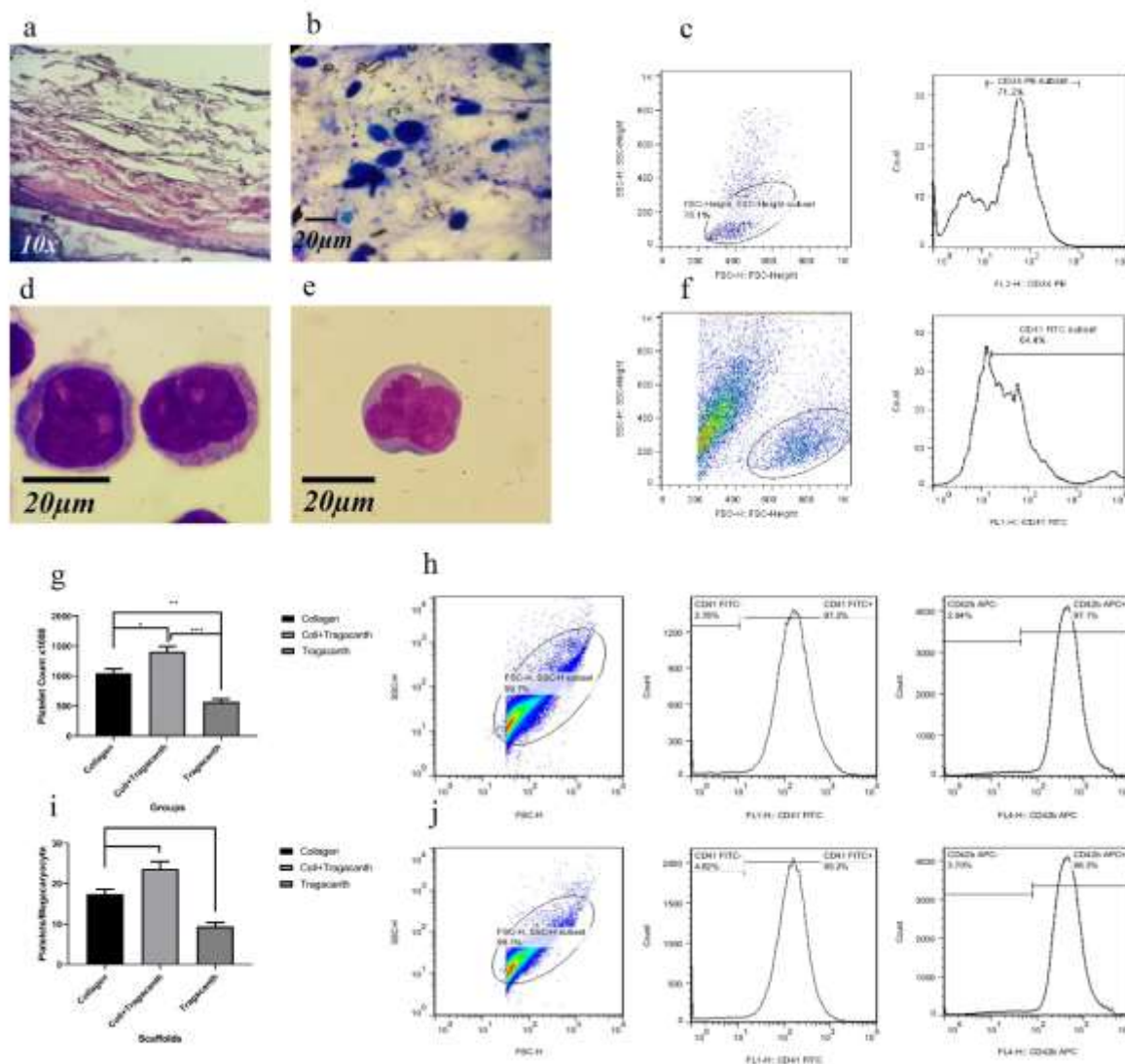


Figure 3. The differentiated MKs produced from UCB-SCs and the flow cytometry results of the final PLTs: a. PLT aggregates (red) in the lower phase of the scaffold section by Hematoxyline-Eosin (HE) staining (10X), b. Trapping the MKs in the upper phase of the collagen scaffold (Giemsa Staining, 40X), c. Flow cytometry results of UCB-SCs, d. Mature MKs in the culture medium (day 11), e. MKs from the cell culture (day 13), f. Flow cytometry results of UCB-SCs derived MKs obtained from the cell culture medium, g. Diagram for comparing the average number of PLTs ($\times 1000$) in different scaffold groups (the analysis of variance showed that the mean number of PLTs $\times 1000$ was statistically significant in different scaffolding groups (p-value < 0.001), h. Flow cytometry results for CD41 and CD42 (the selected markers for bioreactor-derived PLTs), i. Diagram for comparing the average number of PLTs (PLTs per MK) in different scaffold groups (the analysis of variance showed that the mean number of PLTs or PLTs per MK was statistically significant in different scaffold groups, p-value < 0.001), j. Flow cytometry results for CD41 and CD42 in normal healthy donors as positive controls.

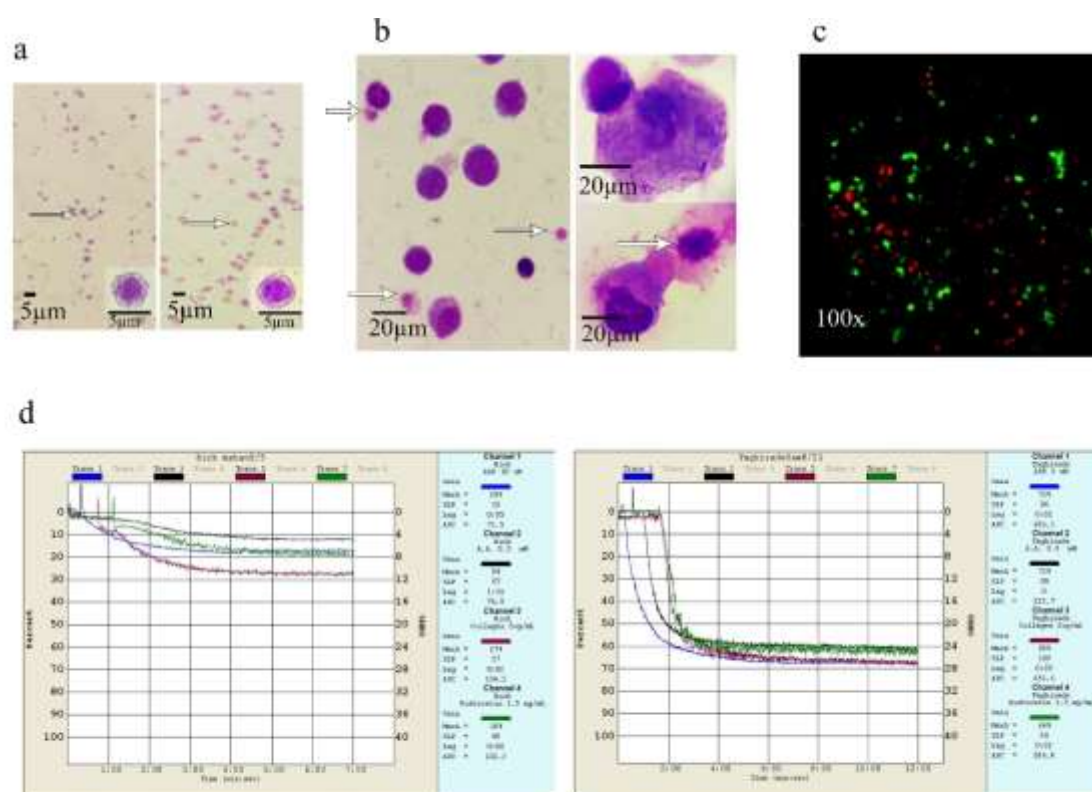


Figure 4. The morphology of the PLTs and pro-PLTs and the results of the functional assessments: a. PLTs produced in the bioreactor (left), PLTs from a normal donor (right), Giemsa staining (100X), b. The morphology of the pro-PLTs on day 13 of culturing (100X), c. Participation of the bioreactor PLTs (green) along with normal donor PLTs (red) in clot forming and PLT aggregation forming under *in-vitro* conditions with fluorescent microscopy (100X), d. Aggregometry results of the bioreactor PLTs (left) and normal donor PLTs (right) in response to PLT activation factors

Discussion

In this study, BM modeling was simulated based on the interaction of MKs with the surrounding extracellular matrix in the corresponding sinusoidal structure. To this end, MKs were placed in the upper layer of the scaffold bilayer structure under shear stress. PLPs were released from the lower layer. They were similar to the natural PLTs released from the BM microenvironment. It has been thought that, due to their low immunogenicity rate and ease of access, UCB-SCs are an interesting source of cells for the production of PLTs. However, in terms of megakaryocytic differentiation, the low lobularity and insufficient differentiation

effectiveness of UCB-SCs limit their application in clinical settings. Since the rate of PLT production is proportional to the ploidy of MKs, UCBs have lower efficacy in PLT production as compared to BM-HSCs (1, 2, 4, 9).

Different research groups have used simulated BM structures with different substrates inside bioreactors to produce PLTs. In a study by Jennifer et al. (33), PLTs were produced from iPSCs in pure collagen scaffolds, but the possibility of unexpected risks restricted their application in clinical trials. Avanzi et al. (20) used differentiated UCB-SCs-derived MKs for the production of PLTs with increased ploidy exposed to Rho kinase

and latrunculin inside a bioreactor with a nanofiber membrane sandwiched between two flow chambers. Although PLT production was enhanced by a rise in ploidy, it was found that rokinase can affect PLT function. Christina et al. (11) tried to produce PLTs in a bioreactor through silk scaffolding loaded with collagen, fibrinogen, fibronectin, and laminin. Despite the promising data, silk limited the quality of the PLT product. Fujiyama et al. (40) used UCB-SC ex vivo xenogeneic BM environment to produce approximately 4 PLTs per MK. Although the BM structure of a pig's thigh bone may be very similar to the mechanism of human PLT production, the findings showed little difference in PLT production with a normal culture medium.

In the present study, UCB-SCs, with such advantages as low immunogenicity, appropriate availability and ease of preparation, were used to produce PLTs. A composite of tragacanth and collagen served as a supportive extracellular matrix for the PLT production inside a bioreactor system. The existence of numerous polysaccharide residues induces a function like that of glycoconjugates-like hyaluronic acid, proteoglycans, and glycoproteins in BM. This increases mutual cell-to-matrix interactions, which are important in megakaryopoiesis and thrombopoiesis processes. According to the results, a significantly higher number of PLTs were produced in the collagen-tragacanth scaffold than in the scaffolds based on collagen or tragacanth alone. Also, fewer PLTs were produced in the pure tragacanth system than in the collagen-based and collagen-tragacanth scaffolds. These findings are attributed to the existence of collagen receptor (GPVI) on MKs and PLTs, which is involved in both binding and activation of mechanisms within MK cells and possibly in PLTs release.

The use of more MK cells, an increased number of the chambers in bioreactors, and an efficient scaffold structure facilitate

the production of sufficient PLTs which, like donor PLTs, can be used to inject into patients with thrombocytopenia. In this regard, attempts were made to produce a large quantity of functional PLTs by constructing a porous scaffold from a combination of collagen and tragacanth and designing a multi-chamber bioreactor without any ploidy manipulation of MKs. If these scaffold and bioreactor are reinforced with extracellular matrix agents, PLT production may increase to a reasonable number for injection. Nowadays, UCB-SCs are considered as an available source of cells, and there are storage facilities in UCB-SC banks. Considering that there are about two million stem cells in each ml of a UCB sample (41) with considerable proliferation capability (18), in this study, the differentiated and proliferated MKs were found to be about 80 times the initial UCB-SCs. Also, about 24 PLTs were produced from each MK in a multi-chamber bioreactor with a collagen-tragacanth scaffold. Totally, the number of PLTs that can be created in a random donor PLT product is from 5.5 to 8.5×10^{10} (42). It is suggested that future studies examine BMSCs for PLT production in the bioreactor system designed here. Besides, the application of the produced PLTs in different thrombocytopenic animal models and clinical trials can help to evaluate the efficiency of in vitro-produced PLTs in comparison with natural PLTs prepared from allogeneic sources.

Conclusion

In this study, a graded porous collagen-tragacanth material was designed and produced for the complex in vitro production of PLTs. This was done by modelling BM distribution and platelet release. In a flow bioreactor, this scaffold was capable of retaining UCB-SC-derived MKs to promote the release of PLTs into an outflow for collection. This procedure provides a prime opportunity to scale up as

it is based on efficient MK production from an available source of CB, a multi-chamber bioreactor, and the biomaterials that are capable of being produced in large amounts.

Acknowledgments

This article is extracted from a PhD thesis registered in Tabriz University of Medical Sciences with number 60432. The authors thank Dr. Jafarzadeh for technical assistance in confocal and transmitting electron microscopy, Dr. Talebi for technical assistance in flow cytometric analysis, Ms. Ameri for cord blood supply, Dr. Dizaji for cooperation in the isolation of UCB-SCs, and Dr. Ahmadinejad from the coagulation laboratory of the Iranian Blood Transfusion Organization for technical assistance in the study of PLT aggregation. The research was supported by the Hematology and Oncology Research Center of Tabriz University of Medical Sciences, the Stem Cell Research Center, and the Department of Anatomy and Histology, Faculty of Medicine, Tabriz University of Medical Sciences.

Conflict of interest

The authors declare no conflict of interest.

References

1. Karagiannis P, Eto K. Manipulating megakaryocytes to manufacture platelets ex vivo. *J Thromb Haemost* 2015;13 (Suppl 1):S47-53
2. Wang B, Zheng J. Platelet generation in vivo and in vitro. *Springerplus* 2016; 5(1):787-797
3. Grozovsky R, Giannini S, Falet H, Hoffmeister KM. Regulating billions of blood platelets: glycans and beyond. *Blood* 2015;126(16):1877-1884
4. Baigger A, Blasczyk R, Figueiredo C. Towards the Manufacture of Megakaryocytes and Platelets for Clinical Application. *Transfus Med Hemother* 2017;44(3):165-173
5. Reems JA, Pineault N, Sun S. In vitro megakaryocyte production and platelet biogenesis: state of the art. *Transfus Med Rev* 2010; 24(1):33-43
6. Thon JN, Medvetz DA, Karlsson SM, Italiano JE Jr. Road blocks in making platelets for transfusion. *J Thromb Haemost* 2015;13 (Suppl 1):S55-62
7. Di Buduo CA, Aguilar A, Soprano PM, Bocconi A, Miguel CP, Mantica G, et al. Latest culture techniques: cracking the secrets of bone marrow to mass-produce erythrocytes and platelets ex vivo. *Haematologica* 2021;106(4):947-957
8. Kotha S, Sun S, Adams A, Hayes B, Phong KT, Nagao R, et al. Microvasculature-directed thrombopoiesis in a 3D in vitro marrow microenvironment. *PLoS One* 2018 ;13(4):e0195082-e0195101
9. Eicke D, Baigger A, Schulze K, Latham SL, Halloin C, Zweigerdt R, et al. Large-scale production of megakaryocytes in microcarrier-supported stirred suspension bioreactors. *Sci Rep* 2018; 8(1):10146-10150
10. Anja B, Dorothee E, Rainer B, Constanca F. Large-Scale Cultures and Bioreactors for the Production of Megakaryocytes and Platelets. *Adv Tech Biol Med* 2017; 5(4):248-252
11. Di Buduo CA, Wray LS, Tozzi L, Malara A, Chen Y, Ghezzi CE, et al. Programmable 3D silk bone marrow niche for platelet generation ex vivo and modeling of megakaryopoiesis pathologies. *Blood* 2015;125(14):2254-2264
12. Liu H, Liu J, Wang L, Zhu F. In vitro Generation of Megakaryocytes and Platelets. *Front Cell Dev Biol* 2021; 9:713434-713444
13. Shaw PH, Gilligan D, Wang XM, Thall PF, Corey SJ. Ex vivo expansion of megakaryocyte precursors from umbilical cord blood CD34+ cells in a closed liquid culture system. *Biol Blood Marrow Transplant* 2003; 9(3):151-156
14. Pineault N, Abu-Khader A. Advances in umbilical cord blood stem cell expansion and clinical translation. *Exp Hematol* 2015;43(7): 498-513

15. Amiri MS, Mohammadzadeh V, Yazdi ME, Barani M, Rahdar A, Kyzas GZ. Plant-based gums and mucilages applications in pharmacology and nanomedicine: a review. *Molecules* 2021;26(6):1770-1793
16. Ono-Uruga Y, Ikeda Y, Matsubara Y. Platelet production using adipose-derived mesenchymal stem cells: Mechanistic studies and clinical application. *J Thromb Haemost* 2021;19(2):342-350
17. Izady E, Saltanatpour Z, Liu LP, Alizadeh A, Hamidieh AA. Toward in Vitro Production of Platelet from Induced Pluripotent Stem Cells. *Stem Cell Rev Rep* 2022;18(7):2376-2387
18. Yaghoubi Y, Hassanzadeh A, Naimi A, Abdolahi S, Yousefi M, Aghebati-Maleki L, et al. The Effect of Platelet Lysate on Expansion and Differentiation Megakaryocyte Progenitor Cells from Cord Blood CD34+ enriched Cells. *Iran J Ped Hematol Oncol* 2021;11(3):172-182
19. Yang J, Luan J, Shen Y, Chen B. Developments in the production of platelets from stem cells (Review). *Mol Med Rep* 2021; 23(1):7-14
20. Avanzi MP, Oluwadara OE, Cushing MM, Mitchell ML, Fischer S, Mitchell WB. A novel bioreactor and culture method drives high yields of platelets from stem cells. *Transfusion* 2016; 56(1):170-178
21. Taghavizadeh Yazdi ME, Nazarnezhad S, Mousavi SH, Sadegh Amiri M, Darroudi M, Bains F, Kargozar S. Gum Tragacanth (GT): A Versatile Biocompatible Material beyond Borders. *Molecules* 2021; 26(6):1510-1528
22. Nejatian M, Abbasi S, Azarikia F. Gum Tragacanth: Structure, characteristics, and applications in foods. *Int J Biol Macromol* 2020;160:846-860
23. Pirbalouti AG, Imaniyan-Fard M. Variation on biological activity and phytochemical characteristics of gum tragacanth exudate from *Astragalus gossypinus* and *A. parrowianus*. *Acta Sci Pol* 2016; 15(3):141-152
24. Ranjbar-Mohammadi M, Bahrami SH. Development of nanofibrous scaffolds containing gum tragacanth/poly (ϵ -caprolactone) for application as skin scaffolds. *Mater Sci Eng C Mater Biol Appl* 2015;48:71-80
25. Nazarzadeh Zare E, Makvandi P, Tay FR. Recent progress in the industrial and biomedical applications of tragacanth gum: A review. *Carbohydr Polym* 2019; 212:450-467
26. Polez RT, Morits M, Jonkergouw C, Phiri J, Valle-Delgado JJ, Linder MB, et al. Biological activity of multicomponent bio-hydrogels loaded with tragacanth gum. *Int J Biol Macromol* 2022;215:691-704
27. Ghayempour S, Montazer M, Mahmoudi Rad M. Tragacanth gum as a natural polymeric wall for producing antimicrobial nanocapsules loaded with plant extract. *Int J Biol Macromol* 2015;81:514-520
28. Liebert MA. Final Report on the Safety Assessment of Tragacanth Gum. *J Am Coll Toxicol* 1987; 6(1):1-22
29. Boamah PO, Afoakwah NA, Onumah J, Osei ED, Mahunu GK. Physicochemical Properties, Biological Properties and Applications of Gum Tragacanth-A Review. *Carbo Pol Tech and App* 2023:100288-100301
30. Davidenko N, Schuster CF, Bax DV, Raynal N, Farndale RW, Best SM, et al. Control of crosslinking for tailoring collagen-based scaffolds stability and mechanics. *Acta biomater* 2015; 25:131-142
31. Yang C. Enhanced physicochemical properties of collagen by using EDC/NHS-crosslinking. *Bull. Mater. Sci* 2012;35:913-918
32. Shepherd DV, Shepherd JH, Ghose S, Kew SJ, Cameron RE, Best SM. The process of EDC-NHS Cross-linking of reconstituted collagen fibres increases collagen fibrillar order and alignment. *APL Mater* 2015; 3(1):014902-014910

33. Shepherd JH, Howard D, Waller AK, Foster HR, Mueller A, Moreau T, et al. Structurally graduated collagen scaffolds applied to the ex vivo generation of platelets from human pluripotent stem cell-derived megakaryocytes: Enhancing production and purity. *Biomaterials* 2018;182:135-144
34. Vučetić D, Ilić V, Vojvodić D, Subota V, Todorović M, Balint B. Flow cytometry analysis of platelet populations: usefulness for monitoring the storage lesion in pooled buffy-coat platelet concentrates. *Blood Transfus* 2018;16(1):83-92
35. Shaiegan M, Ghasemi A, Zadsar M, Ahmadi J, Samiee SH. Human platelet antigens polymorphisms: Association to primary immune thrombocytopenia in the Iranian patients. *Iran J Ped Hematol Oncol* 2021;11(1):41-50
36. Peerschke EI, Castellone DD, Stroobants AK, Francis J. Reference range determination for whole-blood platelet aggregation using the Multiplate analyzer. *Am J Clin Pathol* 2014;142(5):647-656
37. Nagao Y, Masuda R, Ando A, Nonaka M, Nishimura A, Goto K, et al. Whole Blood Platelet Aggregation Test and Prediction of Hemostatic Difficulty After Tooth Extraction in Patients Receiving Antiplatelet Therapy. *Clin Appl Thromb Hemost* 2018;24(1):151-156
38. de Witt SM, Swieringa F, Cavill R, Lamers MM, van Kruchten R, Mastenbroek T, et al. Identification of platelet function defects by multi-parameter assessment of thrombus formation. *Nat Commun* 2014; 5:4257-4270
39. Lu Q, Malinauskas RA. Comparison of two platelet activation markers using flow cytometry after in vitro shear stress exposure of whole human blood. *Artif Organs* 2011;35(2):137-144
40. Fujiyama S, Hori N, Sato T, Enosawa S, Murata M, Kobayashi E. Development of an ex vivo xenogeneic bone environment producing human platelet-like cells. *PLoS One*.2020;15(4):e0230507-e0230519
41. Fumarola S, Lucarini A, Lucchetti G, Piroli L, Pierelli L. Predictors of cord blood unit cell content in a volume unrestricted large series collection: a chance for a fast and cheap multiparameter selection model. *Stem Cell Res Ther* 2022; 13(1):246-256
42. Youk HJ, Hwang SH, Oh HB, Ko DH. Evaluation and management of platelet transfusion refractoriness. *Blood Res* 2022;57(S1):6-10